CZECH TECHNICAL
UNIVERSITY
IN PRAGUE

FACULTY
OF ELECTRICAL
ENGINEERING

DIPLOMA
THESIS

2019

PŘEMYSL MICHAL
VIDNER

CZECH TECHNICAL UNIVERSITY IN PRAGUE

FACULTY OF ELECTRICAL ENGINEERING

Department of Electromagnetic Field

Transmission of Millimeter Waves over Fiber-Optic Infrastructure

Přenos milimetrových vln přes optické infrastruktury

Diploma thesis

Bc. Přemysl Michal Vidner

Supervisor: prof. Ing. Stanislav Zvánovec, Ph.D
Co-supervisor: Ing. Jan Bohata, Ph.D
Prague, May 2019

ZADÁNÍ DIPLOMOVÉ PRÁCE

I. OSOBNÍ A STUDIJNÍ ÚDAJE

Příjmení: **Vidner** Jméno: **Přemysl Michal** Osobní číslo: **434886**

Fakulta/ústav: **Fakulta elektrotechnická**

Zadávající katedra/ústav: **Katedra elektromagnetického pole**

Studijní program: **Elektronika a komunikace**

Studijní obor: **Rádiová a optická technika**

II. ÚDAJE K DIPLOMOVÉ PRÁCI

Název diplomové práce:

Přenos milimetrových vln přes optické infrastruktury

Název diplomové práce anglicky:

Pokyny pro vypracování:

V rámci diplomové práce analyzujte možnosti přenosu milimetrových vln pro 5G systémy přes optické vláknové infrastruktury (Radio over Fiber, RoF) a bezdrátový optický spoj (free space optics, FSO). Zaměřte se zejména na vliv přenášeného frekvenčního pásma a dále pak na specifika jednotlivých přenášených modulačních formátů. V simulátoru a dále pak i experimentálně ověřte generaci milimetrových vln a jejich přenos přes optickou infrastrukturu s potlačením nosné frekvence.
Specialista: Ing. Jan Bohata, Ph.D.

Seznam doporučené literatury:

[1] J. Bohata, M. Komanec, J. Spacil, Z. Ghassemlooy, S. Zvanovec, R. Slavik, 24 - 26 GHz Radio over Fiber and Free Space Optics for 5G Systems, Optics Letters, vol. 43, no. 5, pp. 1035-1038, 2018.
[2] C. H. Lee, Microwave Photonics, 2nd ed. (Taylor & Francis, 2013).

Jméno a pracoviště vedoucí(ho) diplomové práce:

prof. Ing. Stanislav Zvánovec, Ph.D., katedra elektromagnetického pole FEL

Jméno a pracoviště druhé(ho) vedoucí(ho) nebo konzultanta(ky) diplomové práce:

Datum zadání diplomové práce: **04.02.2019** Termín odevzdání diplomové práce: **24.05.2019**

Platnost zadání diplomové práce: **20.09.2020**

prof. Ing. Stanislav Zvánovec, Ph.D. podpis vedoucí(ho) práce	podpis vedoucí(ho) ústavu/katedry	prof. Ing. Pavel Ripka, CSc. podpis děkana(ky)

III. PŘEVZETÍ ZADÁNÍ

Diplomant bere na vědomí, že je povinen vypracovat diplomovou práci samostatně, bez cizí pomoci, s výjimkou poskytnutých konzultací. Seznam použité literatury, jiných pramenů a jmen konzultantů je třeba uvést v diplomové práci.

. | Datum převzetí zadání

Podpis studenta

Acknowledgments

I would like to thank prof. Stanislav Zvánovec for the much valued remarks and the opportunity, Jan Bohata for the lab assistance and guidance, and Jan Spáčil for the help with RF hardware. I would also like to apologize everyone for the broken mini SMP adapter.

I hereby declare that this thesis is my own work, and I cited all sources in accordance with Methodical Guidelines on Adherence to Ethical Policy during Higher Education Thesis Preparation.

Prohlašuji, že jsem předloženou práci vypracoval samostatně a že jsem uvedl veškeré použité informační zdroje v souladu s Metodickým pokynem o dodržování etických principů při přípravě vysokoškolských závěrečných prací.

Prague

V Praze dne:

. . . . . .

Přemysl Michal Vidner

Abstract

The first part of this thesis explores general options for millimeter wave transmission over fiber-optic infrastructure. Further on, it focuses on optical modulation techniques – optical carrier suppression in particular.

Most of this work characterizes experimental millimeter waves over fiber links – components and basic functionality, data transmission, and data transmission through optical carrier suppression link.

Abstrakt

První část této práce je rešerše možností přenosu milimetrových vln přes optické infrastruktury. Práce se dále zaměřuje na optické modulační techniky, obzvláště potlačení optické nosné.

Větší částí této práce je charakterizace experimentálních spojů milimetrových vln přes optická vlákna – jeho součásti a základní funkce, přenos dat a přenos dat skrze spoj s potlačenou optickou nosnou.

Keywords

radio over fiber, RoF, RFoF, microwave photonics, optical carrier suppression, 5G

Klíčová slova

milimetrové vlny, optické vlákno, RoF, RFoF, mikrovlnná fotonika, potlačení optické nosné, 5G

Contents

Nomenclature

5G NR	5G New Radio
BBoF	Baseband over Fiber
CP-OFDM	Cyclic Prefix OFDM
DC	Direct Current
DFT-s-OFDM	Discrete Fourier Transform spread OFDM
DIFoF	Digitized IF over Fiber
DML	Directly Modulated Laser
DWDM	Dense WDM
EAM	Electro-Absorption Modulator
EDFA	Erbium-Doped Fiber Amplifier
FSO	Free Space Optics
IF	Imtermediate Frequency
LNA	Low-Noise Amplifier
LO	Local Oscillator
LTE	Long-Term Evolution
MIMO	Multiple-Input and Multiple-Output
MZM	Mach-Zehnder Modulator
OCS	Optical Carrier Suppression
OFDM	Orthogonal Frequency Division Multiplexing
OSA	Optical Spectrum Analyzer
OSSB	Optical Single Sideband
PA	Power Amplifier
PC	Polarization Controller
PDSCH	Physical Downlink Shared Channel
QAM	Quadrature Amplitude Modulation
QPSK	Quadrature Phase-Shift Keying
RBW	Resolution Bandwidth
RF	Radio Frequency
RFoF	RF over Fiber
RoF	Radio over Fiber

SNR	Signal to Noise Ratio
VNA	Vector Network Analyzer
VOA	Variable Optical Attenuator
WDM	Wavelength Division Multiplexing

Part 1

Introduction

As mobile networks move into millimeter-wave frequencies for wider usable bandwidth hence data rates, it is necessary to deliver the microwave signal over distances for any sort of distributed infrastructures, either picocellular networks or distributed antenna system. Such delivery is impractical using metallic lines due to their high attenuation and costs. Optical infrastructures can be used instead as a high performance system. Transmitting radio frequency (RF) signal over fiber is simply called Radio over Fiber (RoF) or RF over fiber (RFoF).

The very generous bandwidth of an optical system can be used to multiplex many signals into a single line via wavelength division multiplexing (WDM). The low fiber attenuation and availability of fiber amplifiers allow for transmission over large distances. Furthermore, free space optics (FSO) can be used to bridge short distances where the cost of laying optical cables would be prohibitive.

Commercial 40 $^{Gb}/_{s}$ optical components can be used for immediate microwave signal transmission, while frequency up-conversion in both RF or optical domain can be used to transmit even higher frequencies. Photonic technologies can potentially be used to generate microwave carriers up to THz bands, and advanced coherent optical modulations can be used to deliver extremely high-bandwidth signals [1].

The goal of this work is to implement and measure a 25 GHz RoF system, which is a frequency band in consideration for fifth generation (5G) networks. Furthermore, optical carrier suppression technique will be used for RF frequency doubling and potential dispersion fading reduction. The data formats tested for transmission are LTE (Long-Term Evolution) baseband signals, which are still relevant for fifth-generation 5G mobile networks.

First, there will be an overview of relevant technologies. Then, basic functionality of such system will be verified by simulations. After simulations, an actual RoF setup will be measured for basic functionality. Further on, data transmission will be tested for a basic link, and lastly transmission with optical carrier suppression will be tested and compared to the previous setup.

Radio over Fiber is a technology encompassing wide variety of engi-

neering fields: solid state physics, semiconductor technology, photonics, fiber optics, microwave technology, signal propagation, digital communications, and networking. Therefore it incorporates advances in all of these fields. The focus of this work is on practical hardware laboratory implementation of such a system. Therefore the topics will be analyzed in a limited scope.

Part 2

Theory

2.1 Motivation

2.1.1 5G Systems

In order to increase throughput and number of devices served, 5G networks will utilize millimeter waves as carrier frequencies, mainly for outdoor to outdoor transmission [2]. The particular bands will be allocated nationally but the bands under considerations are these [3]: 24.25–27.5 GHz; 31.8–33.4 GHz; 37–40.5 GHz; 40.5–42.5 GHz; 42.5–43.5 GHz; 45.5–47 GHz; 47–47.2 GHz; 47.2–50.2 GHz; 50.4–52.6 GHz; 66–76 GHz; 81–86 GHz.

Specific regional allocations are still under consideration [4], however it seems that there is a wide consensus on the band 24.25–27.5 GHz and good consensus on the bands 31.8–33.4 GHz, and 40.5–42.5 GHz.

The new air interface of 5G networks is called 5G NR (5G New Radio) and is, so far, defined for frequencies from well-established UHF frequencies[1], used as of now for LTE, up to 52.6 GHz [2]. It is an evolution of LTE physical layer and both are expected to work alongside in 5G networks. NR also accounts for carrier frequencies above 6 GHz unlike LTE, and can use up to 400 MHz bandwidth per component carrier. It uses CP-OFDM (cyclic prefix orthogonal frequency division multiplexing) for both downlink and uplink, with possible DFT-s-OFDM (discrete Fourier transform spread OFDM) for uplink. The modulations used for PDSCH (Physical Downlink Shared Channel – user data) are quadrature phase-shift keying (QPSK), and following m-ary quadrature amplitude modulations (m-QAM): 16-QAM, 64-QAM, and 256-QAM – the same case as in LTE physical layer. NR uses different channel coding (polar codes and low-density parity-check codes) dynamic duplexing, and, what is interesting for our work, beamforming for millimeter waves, that means directional radio wave is to be expected.

[1] 300 MHz – 3 GHz

2.1.2 Transmission Medium

The primary motivation for transmitting microwave signals over optical fiber is how well an optical fiber performs compared to a coaxial line. Consider a Pasternack 2.21 millimeter low loss coaxial cable with copper inner and outer conductor with a quality PTFE dielectric [5]. Its attenuation at 26.5 GHz is 3.14 dB/m and its price is $31/m. It is essentially useless over distances larger than a few meters therefore the transmitter needs to be in a close vicinity of the antenna.

A WR42 waveguide has an acceptable attenuation of about 0.4 dB/m, but its prices are orders of magnitude higher and it is unwieldy.

A Corning SMF-28 single mode fiber [6] has a nearly negligible attenuation (0.2 dB/km at 1550 nm), and it's considerably cheaper $3.3/m. RoF (and similar systems) therefore allow detaching the antenna from the base-station and/or control unit, which is useful for any sort of distributed infrastructure like pico-cellular networks [7], distributed antenna systems [8], and MIMO (multiple-input and multiple-output).

Another advantage is that RoF makes free-space optics links between buildings, where optical fiber installation would be expensive, easy to use with good bitrates [9].

2.2 Elementary Setup

Radio over fiber is, in essence, a very simple system: An already modulated RF signal is modulated on a coherent optical carrier via a kind of optical modulator: Mach-Zehnder amplitude modulator (MZM), electro-absorption modulator (EAM), directly modulated laser (DML) or alternatively a phase modulator. The RF signal is reconstructed at the receiving end by simple detection on a photodiode (in case of amplitude modulation). The signal is amplified and either radiated out (in case of transmitter) or processed (in case of receiver). An example setup can be seen in Fig. 2.1.

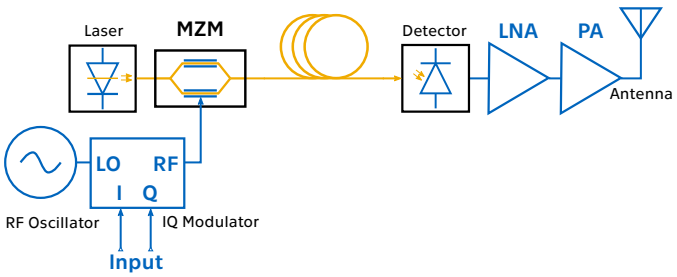

Figure 2.1: An example RF setup. MZM – Mach-Zehnder modulator, LNA – Low noise amplifier, PA – Power amplifier

2.3 Modes of Transmission

There are multiple ways of delivering the RF signal between the source and the antenna [10].

- Baseband over fiber (BBoF)
  - Baseband signal is transmitted. Detected signal is then modulated on a RF carrier from an oscillator at the receiving side.
- Digitized IF over fiber (DIFoF)
  - Baseband signal modulated on a intermediate frequency is digitized and transmitted digitally over the fiber. Detected signal is converted to analog domain and up-converted to carrier frequency.
- Digitized radio over fiber (DRFoF)
  - RF signal is digitized and transmitted digitally over the fiber. Detected signal is converted to analog domain.
- Sigma-delta modulated signal over fiber (SDoF) [11]
  - RF signal undergoes sigma-delta modulation and is transmitted. Detected signal is filtered, and amplified.
- Intermediate frequency over fiber (IFoF)
  - The baseband signal modulated on a intermediate frequency is modulated on a optical carrier. Detected signal is amplified and upconverted to carrier frequency.
- Radio over fiber (RFoF)
  - RF signal is modulated upon an optical carrier. The detected signal is amplified.

Different systems impose different requirements upon digital, RF, and optical domain. RFoF is the simplest one from the RF perspective, but requires wideband optical components (photodiode, modulator). BBoF isn't demanding on the optical side, but requires complete RF circuitry at the antenna. Digital approaches ease the demands on the optical side (distortion and nonlinear characteristics of the optoelectronic components), but require powerful analog-to-digital and digital-to-analog converters. IF approaches ease the bandwidth demands on the optical (and/or digital in case of DIFoF) components, but require frequency conversion in the RF domain.

Phase modulation, instead of amplitude modulation, in the optical domain is an option over dispersive media (i.e. multimode fibers) [12].

The use of systems described above is standardized in ITU-T G.55 [13]. Although it is fairly general, it describes architectures and network models of the systems summarized above, plus more interestingly it provides

example of LTE over fiber system performance evaluation. The example will be used as a starting point our for measurements later.

2.4 Millimeter Waves over Fiber

While the optical fiber transmission of mm-waves brings the advantage of low losses, the fiber dispersion is an issue at such modulation frequencies. As two in-phase RF modulation sidebands are generated in case of amplitude modulation, the RF signal is subject to dispersion. The resulting effect is dispersion fading as such: [14]

$$P_{RF} \propto \cos^2\left(\frac{\pi LD}{c}\lambda_c^2 f_{RF}^2\right) \tag{2.1}$$

where L is the fiber length, D is the dispersion (in $\mathrm{ps}\cdot\mathrm{nm}^{-1}\cdot\mathrm{km}^{-1}$), λ_c the wavelength of the optical carrier, c the speed of light, and f_{RF} the RF signal frequency. The dispersion fading can be as strong as 35 dB [14]; the effect can be seen in Fig. 2.2. To overcome this problem, either optical single sideband (OSSB) modulators can be used, or optical double- or single-sideband suppresed-carrier technique can be used [14].

Using optical infrastructure with millimeter waves has also other advantages. Optical techniques can be used for generation of mm-wave signals. With two lasers, optical phase-locked loop can be used to generate mm-wave carriers [15]. The other technique is to bias a Mach-Zehnder amplitude modulator to its zero-bias point which achieves frequency doubling and dispersion fading reduction as described before [16]. This option is further examined in section 2.6 on page 15.

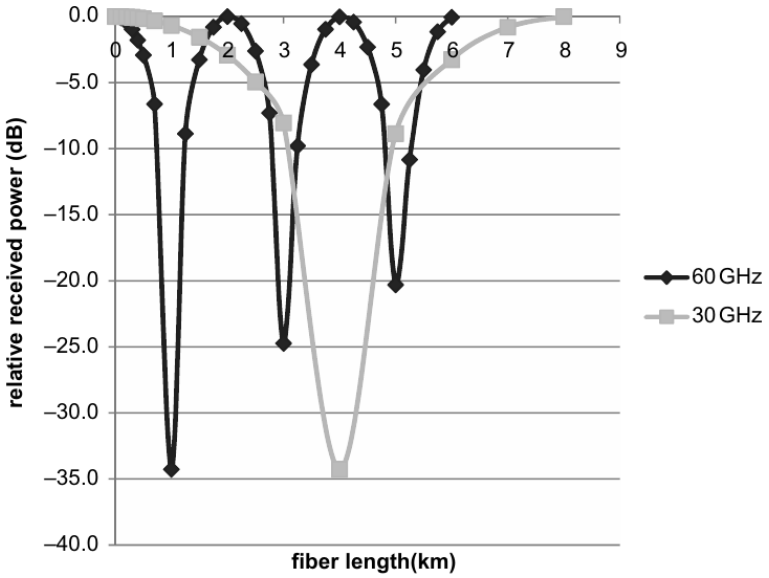

Figure 2.2: mm-wave over fiber dispersion fading, taken from [14]. λ_c = 1550 nm, $D = 17\,\mathrm{ps}\cdot\ \mathrm{nm}^{-1}\cdot\mathrm{km}^{-1}$

2.5 Modulator Choice for RoF

2.5.1 Directly Modulated Laser

Direct modulation works very simply by modulating the driving voltage of a laser diode. The main advantage of this approach is its low cost and simplicity. However, its bandwidth is limited by package or mount parasitics, chip parasitics, and intrinsic laser limitations [17]:

Chip and mount parasitics are caused by resistances, capacitances, inductances (and resonances of these) of the physical realization of the diode chip and package. These can be suppressed to a degree by miniaturization and advanced manufacturing techniques. Intrinsic laser limitations stem from various mechanisms such as: spontaneous emission coupled into the lasing mode, spatial hole burning combined with carrier diffusion, nonlinearities due to spectral hole burning and nonlinear two-photon absorption. These can be summarized as damping from spontaneous emission and damping from gain compression. These are largely dependent on output power and population inversion threshold current, hence the frequency response of a directly modulated laser diode depends on driving current. The higher the output power and the lower the temperature is the higher the 3 dB bandwidth is. In addition to damping, the bandwidth is further limited by frequency chirp [18].

The bandwidth of DML is usually limited at 20 GHz, but it offers linear modulation response, unlike Mach-Zehnder modulators [9].

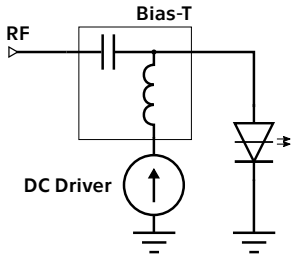

Figure 2.3: Directly modulated laser diode

2.5.2 Electro-Absorption Modulator

Electro-absorption (EA) modulators are semiconductor devices. The band gap is engineered so that the material is transparent at the signal's wavelength. When a voltage is applied across the n-p junction, the band gap moves to the photon energy level and it starts absorbing photons (Franz-Keldysh effect) hence creating photocurrent, similar to a photodiode. Its transfer function is

$$E_0(t) = \exp\left(-\frac{\Delta\alpha[V(t)]}{2}L - j\Delta\beta[V(t)]L\right). \tag{2.2}$$

$\Delta\alpha[V(t)]$ is power attenuation coefficient, $\beta[V(t)]$ is phase coefficient (hence frequency chirp) and L is the length of the modulator. Both coefficients

are strongly nonlinear. Therefore its performance is not as good as Mach-Zehnder modulator. EA modulators can be, however, easily integrated into laser diode chips as they are semiconductor devices and do not require $LiNbO_3$ integrated optics.

2.5.3 Mach-Zehnder Modulator

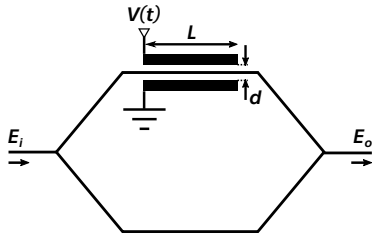

Figure 2.4: Single electrode Mach-Zehnder modulator.

Mach-Zehnder modulator (MZM) is a Mach-Zehnder interferometer with one or both arms phase modulated by Pockels effect, that is: in some crystals, the refractive index of the material is linearly proportional to the electric field applied, which can be exploited for phase modulation [18]:

$$\phi(V) = \left(\frac{2\pi\alpha_{EO}L}{\lambda d}\right)V \tag{2.3}$$

where ϕ is the resulting phase shift, α_{EO} is the linear electro-optic coefficient of the material, L the length of the electrodes, λ wavelength of the light, d distance between electrodes, and V applied voltage.

The transfer function of a Mach-Zehnder interferometer is

$$P_o = P_i \cos^2\left(\frac{\phi_1 - \phi_2}{2}\right). \tag{2.4}$$

where P_o is output optical power, P_i input power, and ϕ_1, ϕ_2 phases of the two optical waves when interfering.

Substituting the phase difference with the phase shift caused by phase modulation (Eq. 2.3) and all constants with V_π (voltage required to shift the phase by 180°) yields, in case of single phase modulator (Fig. 2.4), following relation [18]

$$P_o(V) = P_i \cos^2\left(\phi_0 + \frac{\pi V}{2V_\pi}\right).$$

ϕ_0 is the initial phase shift. It is varies by device and can be offset by DC bias. The transfer function is linear only around its quadrature point $V_{\pi/2}$,which means the MZM needs DC biasing.

A hindrance of the single electrode MZM is that it induces frequency chirp. As phase modulation efficiency is independent of DC bias, the amplitude modulation efficiency is not. This can be overcome with dual electrode MZM (Fig. 2.5), fed in push-pull mode $V_1 = -V_2$. The phase modulation in this case is antisymmetric and thus it cancels out. MZM is dependent on polarization hence also polarization control is needed.

MZMs can be manufactured for high bandwidths, but its non-linear nature is an issue for modulating analog signal, which is the case of RoF.

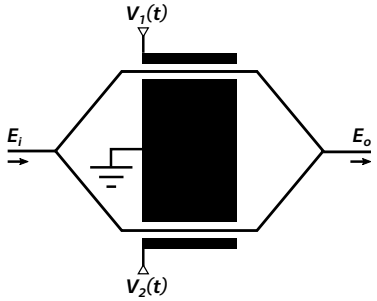

Figure 2.5: Dual electrode Mach-Zehnder modulator

2.6 Optical Carrier Suppression

Amplitude modulation of the optical signal can be used not only for the modulation itself but also to upconvert electric signals. It works as follows [16]: A MZM is biased at $V_{\pi/2}$ and driven by an RF local oscillator (LO) carrier. This signal is further modulated by an intermediate frequency (IF) carrier containing data in an ordinary fashion. The resulting optical intensity is [16]:

$$\begin{aligned} I_{out} = \frac{I_0}{2}[1 + k\cos\omega_{IF}t - 2J_1(m)\cos\omega_{LO}t \\ + kJ_1(m)\cos((\omega_{LO} - \omega_{IF})t) \\ + kJ_1(m)\cos((\omega_{LO} + \omega_{IF})t) \end{aligned} \tag{2.5}$$

where I_0 is optical carrier intensity, m is the modulation index and J_1 is the first-order Bessel function of the first kind. Similar result is found by Sun et al. [19]

This way the IF signal is upconverted to $\omega_{LO} \pm \omega_{IF}$ – we achieve RF mixing in optical domain. In order to achieve further upconversion, the LO MZM needs to be overdriven in order do generate further harmonics and biased so that carrier and even-order optical sidebands are suppressed [20]. This way we achieve both RF mixing and frequency upconversion.

OCS can be intuitively understood like this (see Fig 2.6 on the next page): The first MZM is biased at its zero transmission point, and the modulation voltage (at f_{LO}) is high so even order harmonics including the carrier (f_γ) are suppressed. At the second MZM all the harmonics are modulated by f_{IM}. At the detection photodiode a $2f_{LO}$ RF signal modulated by f_{IM} is generated by beating of the upper and lower optical sidebands separated by $2f_{LO}$ [21].

Optical carrier suppression (OCS) is measured as optical carrier suppression ratio which is a difference (in dB) of power level of the modulated sidebands to the optical carrier.

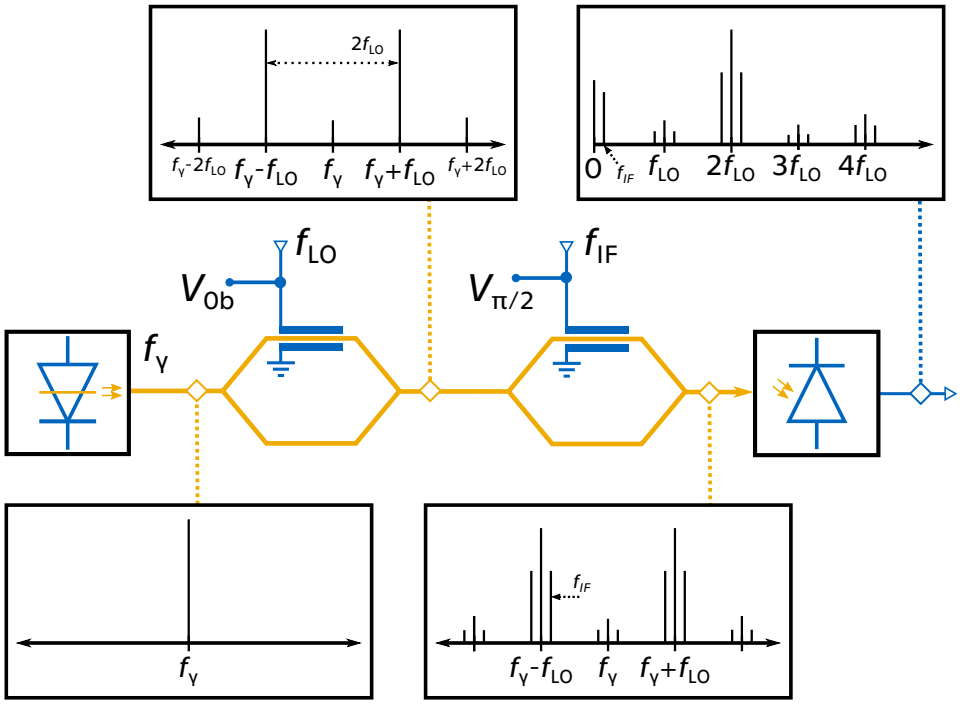

Figure 2.6: Optical carrier suppression principle

2.7 Free Space Optics

Optical infrastructure can be conveniently used to transmit signal over short distances via a laser beam. This could be particularly useful for example for transmission between buildings [9], because optical spectrum usage is not regulated unlike microwave frequencies.

An optical beam coming out of the fiber end is collimated with a set of lenses, transmitted through air and then coupled into fiber at the other end. The advantage of FSO over microwave point-to-point links is essentially unlimited bandwidth, low power losses due to free space losses (inverse square law – losses are minimal thanks to low beam divergence), ease of deployment with existing fiber infrastructure, and already mentioned licence-free operation. The downside is that FSO links are highly susceptible to atmospheric conditions. Fog in particular causes huge fading (as much as 315 dB/km in dense fog [22]), and atmospheric turbulences cause beam misalignment (resulting losses of 4 dB in moderate turbulence [22]). Eye safety is also an issue for higher powers.

Part 3

Measurements and Simulations

3.1 Initial Simulations

3.1.1 Direct Transmission

To assess basic functionality, simulations of a RoF system in Optiwave Optisystem were done. The carrier frequency was 25 GHz. The modulator was a generic $LiNbO_3$ dual-drive MZM. The laser was a generic CW laser at 194.3 THz with 10 MHz linewidth at 5 dBm. There was a path of 5 km single mode fiber. The detector was a InGaAs PIN diode. The simulation setup can be seen in Fig. 3.1 on the following page

As the (extremely) high bandwidth scenario 64QAM modulation at 6 $^{Gb}/_{s}$ with bandwidth of 2 GHz was chosen. As the low bandwidth scenario 8DPSK at 60 $^{Mb}/_{s}$ with bandwidth of 20 MHz was chosen.

The optical spectra can be seen in Fig. 3.2 on the next page. Fairly strong second harmonics of the RF signals are generated in both cases. Higher bandwidth significantly increases the noise floor of the optical signal, and there seems to be a frequency downshift at the second harmonic of the RF signal. The wider bandwidth also means lower carrier suppression can be achieved.

The spectra of the detected RF signals can be seen in Fig. 3.3 on page 19. The frequency downshift of the high-bandwidth signal is noticeable even here. The low-bandwidth signal, however, seems to have a parasitic notch at 23 GHz which also applies to its second harmonic.

3.1.2 Suppressed Carrier Transmission

Behavior of the system in suppressed carrier transmission was simulated as well. A baseband signal was modulated upon an intermediate frequency (16QAM, 20 MHz band, 100 MHz IF). First, the optical carrier was modulated by a half-frequency 12.5 GHz LO signal on the first (carrier) MZM overdriving it. Then, the IF signal was modulated upon the optical carrier on the second (data) MZM.

The bias of the first was set manually to achieve maximal suppression of both carrier and 3rd and higher order products. Second (data) MZM

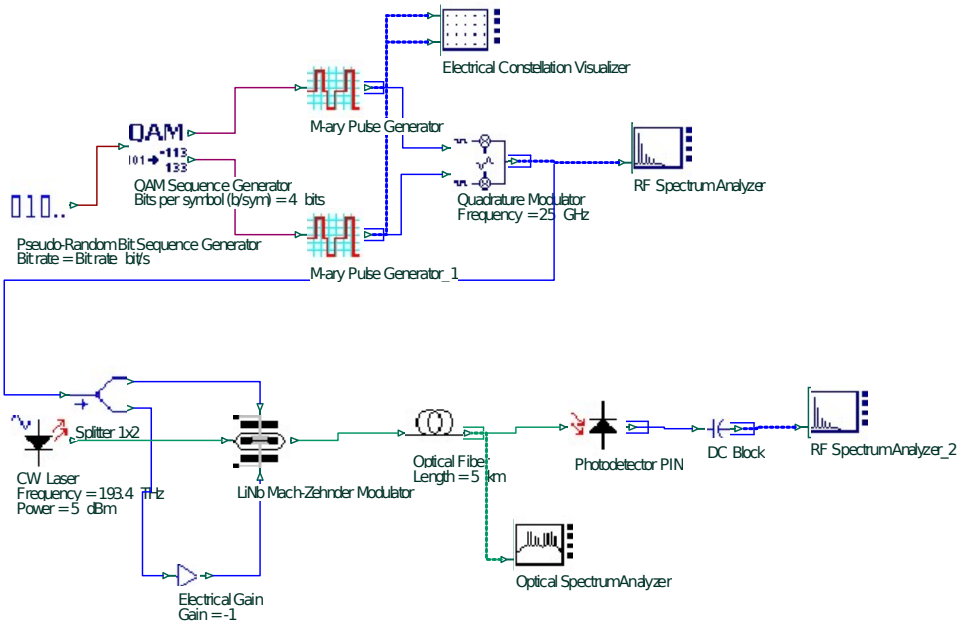

Figure 3.1: Direct transmission simulation setup

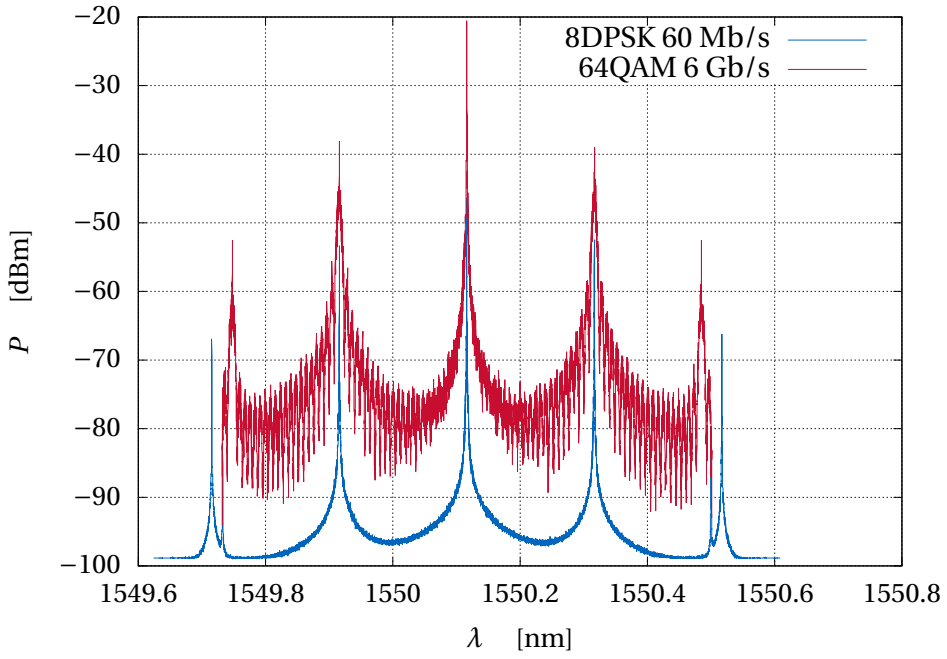

Figure 3.2: Simulated optical spectra

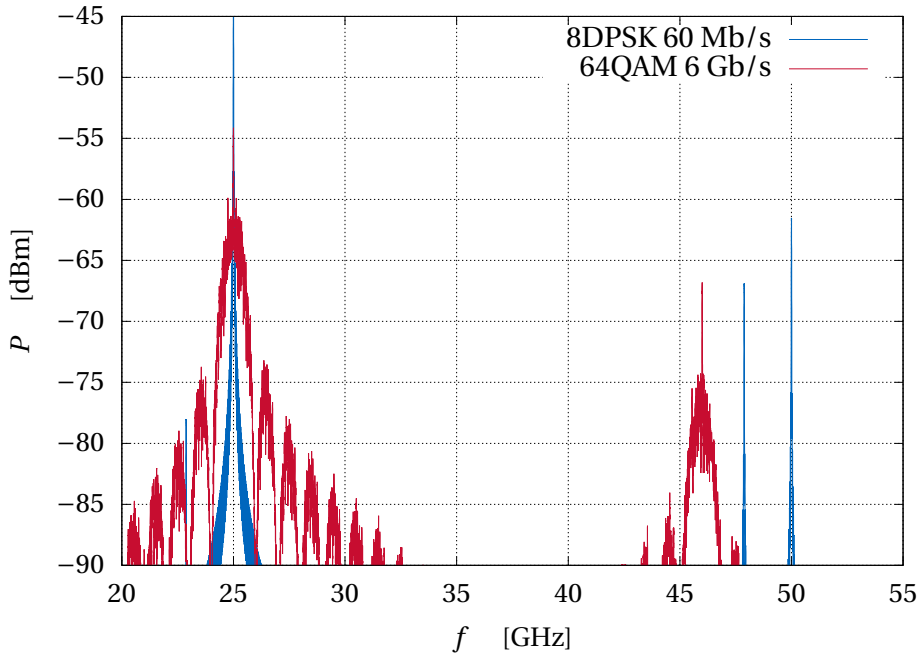

Figure 3.3: Simulated detected RF spectra

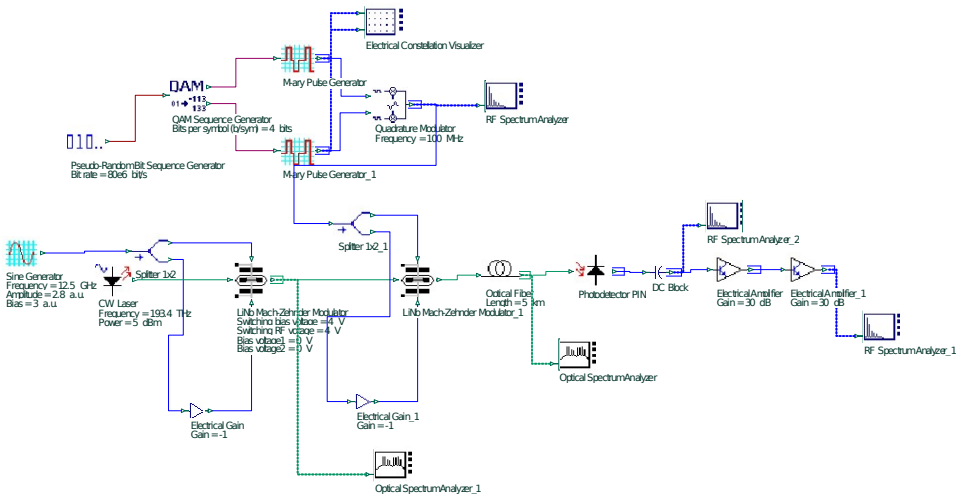

Figure 3.4: Suppressed carrier transmission simulation setup

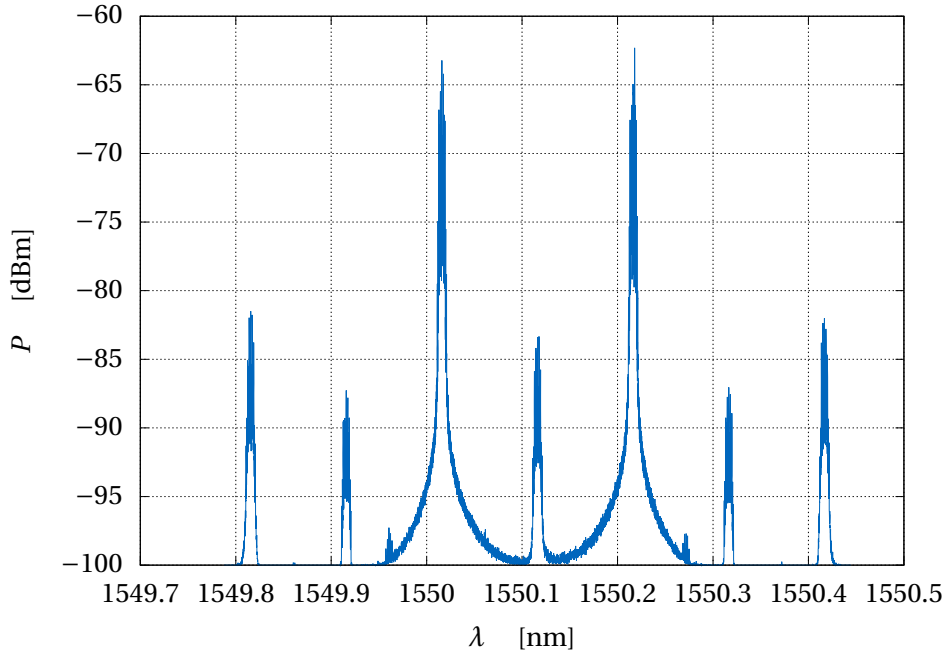

Figure 3.5: Simulated carrier suppression optical spectrum

was biased to its quadrature point.

See Fig. 3.5 for the optical spectrum, which shows the 1550.12 nm IF modulation-widened laser line below the sidebands shifted by 0.1 nm. That is 20 dB optical carrier suppression. Also note higher order products (0.2 and 0.3 nm shift) which give rise to 37.5 GHz, and 50 GHz products in the RF domain.

The RF spectrum (Fig. 3.6 on the facing page) shows fundamental frequency suppression of 20 dB – the same value as in the optical domain. The IF signal of 100 MHz is still present and 5 dB stronger than the upconverted signal.

However, the drawback of this simple approach with an IF signal is that the power of the detected baseband signal is reduced. Firstly, the baseband power is split into two sidebands of which only one is detectable. Otherwise, the suppression is not perfect and significant amount of power remains at the 100 MHz IF. Hence an additional need for filtering and amplification.

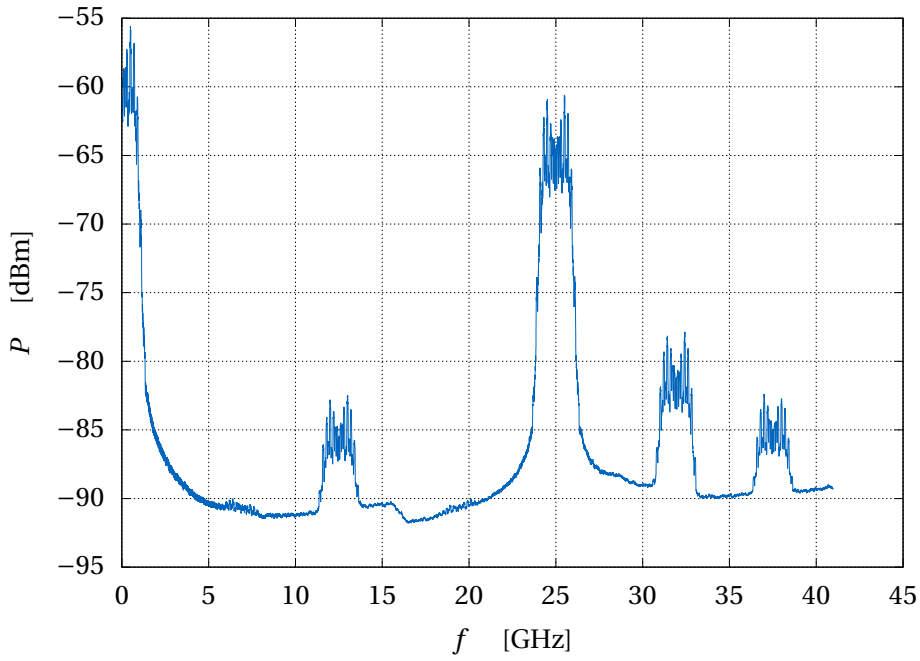

Figure 3.6: Simulated carrier suppression detected RF spectrum

3.2 Characterization of Modulators and Detector

All the setups are based on 40 Gb/s telecommunication components, which should yield satisfying frequency responses up to 40 GHz in all cases.

Basic setups based on all three kind of modulators were considered and experimentally characterized. The detector is in all cases PD-40-C – a 40 GHz InGaAs PIN photodiode. Its measured performance at 1550 nm (see Fig. 3.7 on the next page for $|s_{21}|$) is comparable to the nominal one.

The MZM setup is based on Fujistsu FTM7938 – a 40 Gb/s single drive MZM. The response as per datasheet drops off by frequency, but it should be very well usable up to 30 GHz. The laser in this setup is ID Photonics Cobrite DX-4 tunable laser.

The EAM setup is based on OKI OL5157 1550 nm 40 Gb/s EAM integrated DFB laser. The manufacturer doesn't provide frequency response of the component.

The DML setup is based on a state-of-the art 40 Gb/s DML – a buried heterostructure 1550 nm passive feedback laser [23]. It should show good performance up to 25 GHz and satisfying performance up to 35 GHz, which should make it actually comparable to the other kinds of modulator.

These setups without an actual fiber path, radio transmission etc. were measured on a vector network analyzer (VNA – Rohde & Schwarz ZVA 40) to get frequency response of the modulators (see Fig. 3.8 on page 23. The frequency responses off all setups is satisfying up to 40 GHz. MZM and EAM yield comparable results, while DML is also very wideband with no-

ticeably worse performance due to limited laser power (4.8 dBm). This could be remedied by using an erbium-doped fiber amplifier (EDFA).

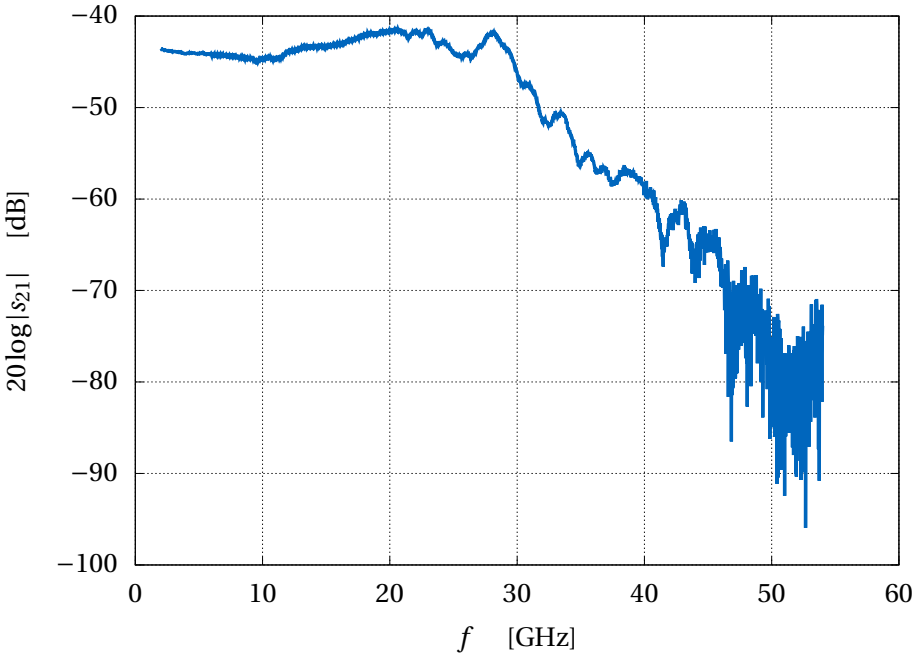

Figure 3.7: Frequency response of the detector (PD-40-C)

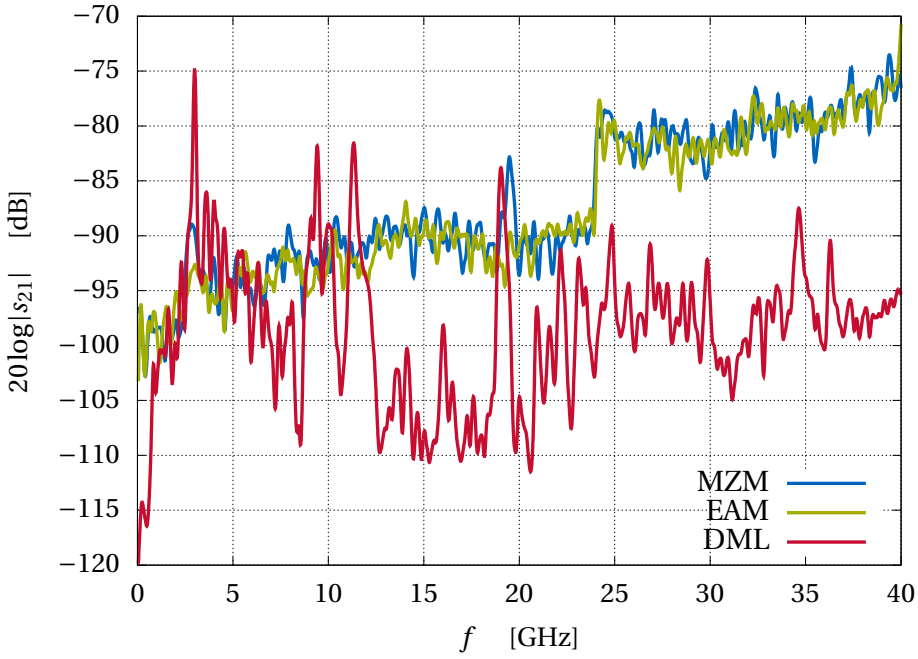

Figure 3.8: Frequency responses of the modulators

3.3 Basic RoF Link Measurement

The RF signal was modulated upon a 1550 nm optical carrier from the above mentioned DML (about 4.8 dBm). The optical signal was then brought over a simple short 2 m free-space optics link – simply focused with a f = 50 mm plano-convex lens at both the receiving and the transmitting side. Then it was coupled to a 1 km SMF-28 fiber path, and amplified by a Keopsys KPS-BT2-C-10-LN-SA EDFA (15 dB gain). The signal was detected on the above mentioned PIN photodiode (biased at 5 V). Then amplified by a low-noise amplifier (Miteq AMF-4F-260400-40-10p) then again by a wide-band medium power amplifier (Analog Devices HMC1131). The microwave signal was further transmitted over 3.6 m RF link by a double-ridged horn antenna (RF Spin DRH40) and detected by the same type. The measurement was carried out on a VNA (Rohde & Schwarz ZVA 40).

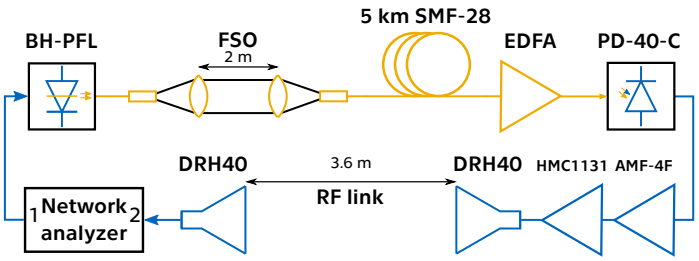

Figure 3.9: Measured RoF Link

A schematic of the setup can be seen in Fig. 3.9 on the previous page. The measured transmission ($20\log|s_{21}|$) is shown in Fig. 3.10. The link is limited by gain of the amplifiers (see Fig. 3.11 on the next page for amplifiers gain) – it shows good performance from 22 GHz up to 33 GHz. There seems to be little limitations on the optical side of the setup as far as simple RF carrier transmission goes.

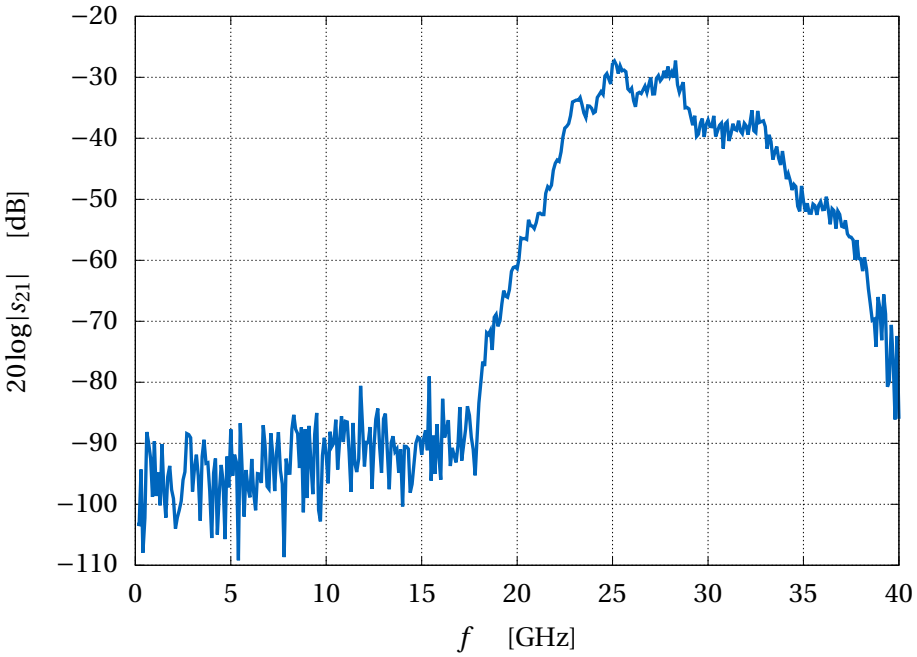

Figure 3.10: Setup transmission

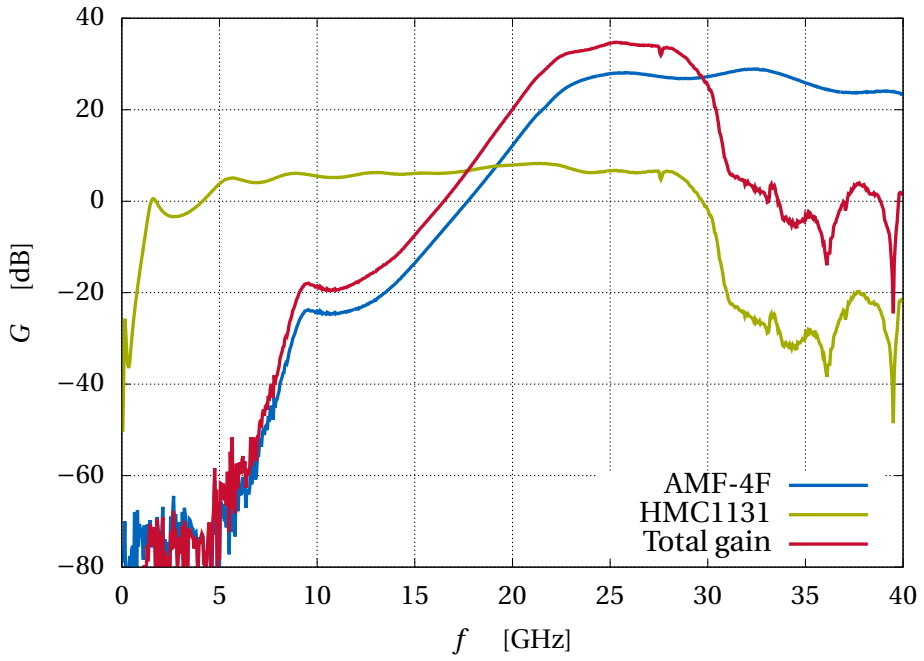

Figure 3.11: RF Amplifiers gain

3.4 Used Transmission Measurement Test Model

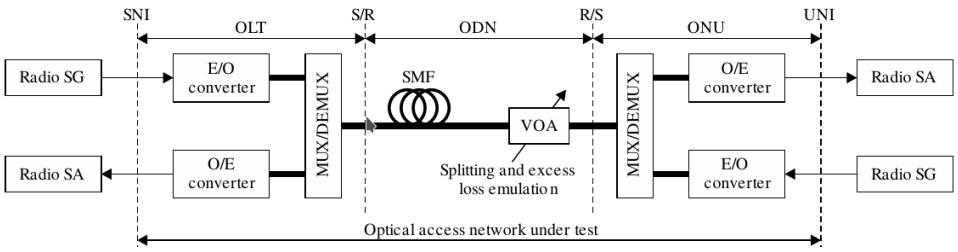

Figure 3.12: General test model for RoF transmission over ODN, as in [13].

Following measurements were based on ITU-T G.55 recommendation [13] as outlined before. As shown in Fig. 3.12, the measurement set-up consists of two radio signal generators (SGs), two radio signal analyzers (SAs), two electric-to-optical (E/O) converters, two optical-to-electric (O/E) converters, two multiplexers / demultiplexers (MUX/DEMUX), a single-mode fiber, and a variable optical attenuator (VOA). The VOA accounts for signal splitting and other excess losses. In our case, however, we are testing the link only in the downlink direction; hence there is essentially no need for optical multiplexing, although multiplexers are included in the more refined setup with optical carrier suppression 3.6 on page 32. Particular devices used are described in the respective sections.

The figure of merit measured is error vector magnitude (EVM), as per "LTE E-UTRA BS radio transmission and reception" (3GPP TS 36.104) [24] and "LTE E-UTRA BS conformance testing" (3GPP TS 36.141) [25].

The error vector magnitude is the length of the vector at the detected symbol location which connects the I/Q reference-signal vector to the I/Q measured-signal vector. [26] It is defined in the constellation space as such:

$$\mathrm{EVM}(\%) = \frac{\sqrt{\frac{1}{N}\sum_{n=0}^{N-1} I_{err}[n]^2 + Q_{err}[n]^2}}{\sqrt{P_{ref}}} \cdot 100 \tag{3.1}$$

where n is detected symbol index, N number of symbols, I_{err} difference between symbol reference and actual value in the I coordinate in the constellation diagram, Q_{err} analogous to I_{err}, P_{ref} power reference.

Documents mentioned above stipulate EVM limits for baseband signal modulations of QPSK: 18.5%, 16-QAM: 13.5%, 64-QAM: 9%, and 256-QAM: 4.5%. 3GPP TS 36.141 [25] provides test models for such measurements. Following test models for signal quality are to be used:

TM 3.1 EVM of 64-QAM modulation

TM 3.1a EVM of 256-QAM modulation

TM 3.2 EVM of 16-QAM modulation

TM 3.3 EVM of QPSK modulation

3.5 Measurement of RoF Link Transmission

As the setup showed good response in the RF domain it was further tested for data transmission.

3.5.1 Setup

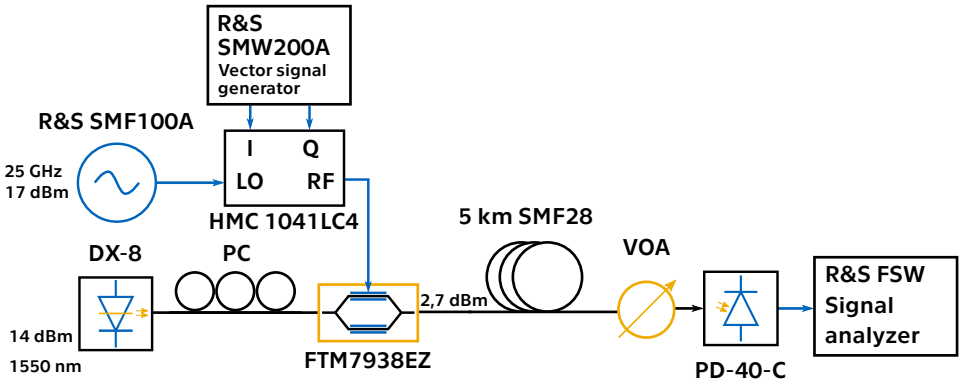

Figure 3.13: RoF transmission link and measurement setup

This setup includes MZM plus Cobrite DX-4 distributed feedback laser instead of directly modulated laser as it has better performance and is easier

to control. The RF and FSO link together with EDFA is excluded for simplicity.

The data symbols are generated on the vector signal generator, then modulated upon the 25 GHz microwave carrier which is then modulated upon a 1550 nm optical carrier on a 40 Gb/s MZM. The MZM was biased at its maximum transmission point at 1.2 V. The optical channel consists of 5 km SMF28 fiber. There is a variable optical attenuator (VOA) to measure the system under various signal to noise ratio (SNR) conditions. The signal is detected on the previously used PIN photodiode. The detected RF signal is directly fed into FSW signal analyzer. The analyzer has a preamplifier so no RF amplification is needed.

See Fig. 3.13 on the facing page for particular device configuration and power budget. The measuring equipment is as follows:

- Cobrite DX-4 DFB tunable laser
- Manual polarization controller (PC)
- Fujitsu FTM7938EZ 40 Gb/s MZM
- PD-40-C PIN photodiode
- HMC 1041LC4 17–27 GHz IQ mixer

The measurement devices are these:

- Rohde & Schwarz SMF100A Microwave signal generator
- Rohde & Schwarz SMW200A Vector signal generator
- OZ Optics Digital variable optical attenuator (VOA)
- Rohde & Schwarz FSW Signal and FFT spectrum analyzer
- Rohde & Schwarz SMP Spectrum analyzer

Figure 3.14: Laboratory RoF transmission link: 1 – 5 km fiber; 2 – SMF100A RF generator; 3 – SMW200A vector signal generator; 4 – FSW signal analyzer; 5 – Polarization controller; 6 – Variable optical attenuator; 7 – FTM7938EZ MZM; 8 – HMC 1041LC4 mixer; 9 – PD-40-C photodiode

3.5.2 RF Domain Measurements

Firstly the generator, Rohde & Schwarz SMF100A, on its own was measured for phase noise on a spectrum analyzer (Rohde & Schwarz FSP) as documented in [27]. The procedure is as follows: set a low resolution bandwidth (RBW – 10 Hz in our case), measure the power of the carrier (P_C), then measure power at specified offset ($P\,(100\,\text{Hz})$ – 100 Hz in this case, as the oscillator has very good purity), finally subtract correction for resolution bandwidth ($10\log(\text{RBW})$)

$$P_{SSB}\,(100\,\text{Hz}) = P\,(100\,\text{Hz}) - P_C - 10\log(\text{RBW}) \tag{3.2}$$

The single sideband phase noise at 100 Hz ($P_{SSB}\,(100\,\text{Hz})$) of the generator was measured to be -60.2 dBc which is close to the datasheet value of -65 dBc [28]. Then the 100 Hz phase noise of the RF carrier after modulation and detection (see Fig. 3.15 on the next page for spectrum) was measured to be -57.9 dBc, which is only a marginal degradation. Therefore the carrier phase noise performance is degraded only slightly by the optical channel.

The spectrum of the carrier modulated with 20 MHz 64-QAM (TM 3.1) was measured (see Fig. 3.16 on the facing page: it shows an ordinary QAM spectrum with rectangular window as it was expected.

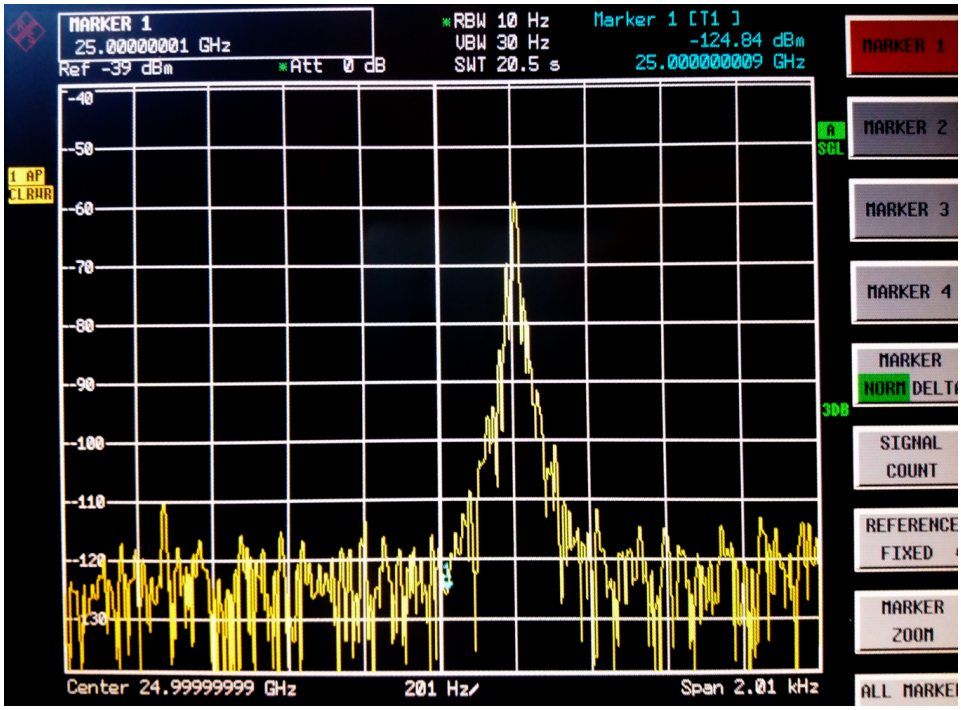

Figure 3.15: RF carrier spectrum after detection on the photodiode

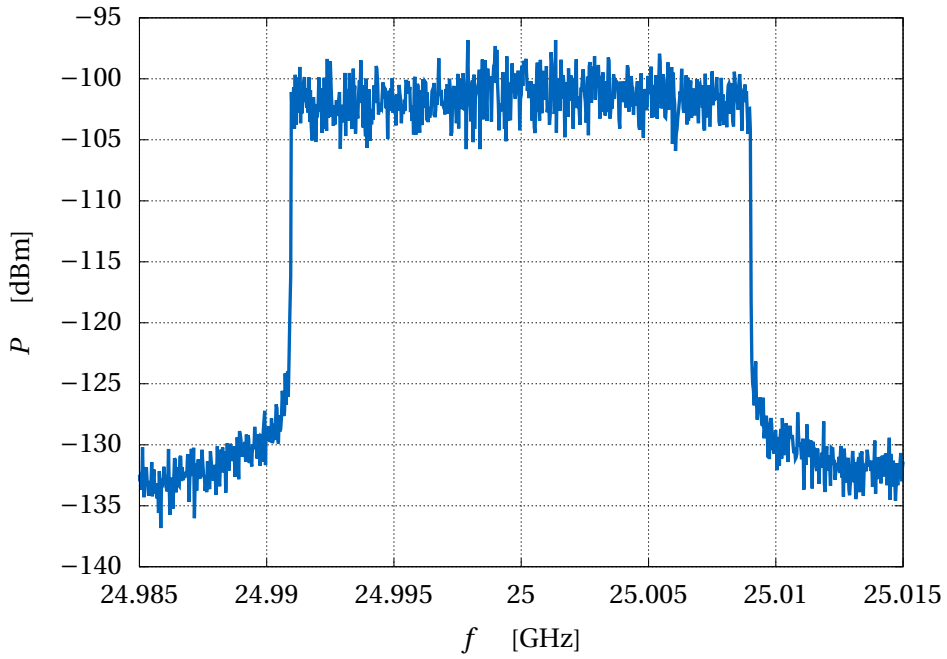

Figure 3.16: Measured 20 MHz 64-QAM RF spectrum

3.5.3 Modulation and Bandwidth

The transmission tests consisted of EVM measurements of transmissions with modulation bandwidths 5, 10, 15 and 20 MHz using QPSK, 16-QAM, 64-QAM, and 256-QAM. The baseband signal was synthesized by Rohde & Schwarz SMW200A. The data were pseudorandom binary sequences using E-UTRA test models 3.1 (64-QAM), 3.1a (256-QAM), 3.2 (16-QAM), and 3.3 (QPSK). The variable optical attenuator was used to vary the received signal power level and set different SNR.

EVM as a function of received power level for 64-QAM with various bandwidths can be seen in Fig. 3.17. The 8% threshold for 64-QAM nominal transmission is reached as follows:

5 MHz -72.8 dBm

10 MHz -69.5 dBm

15 MHz -67.2 dBm

20 MHz -67.7 dBm

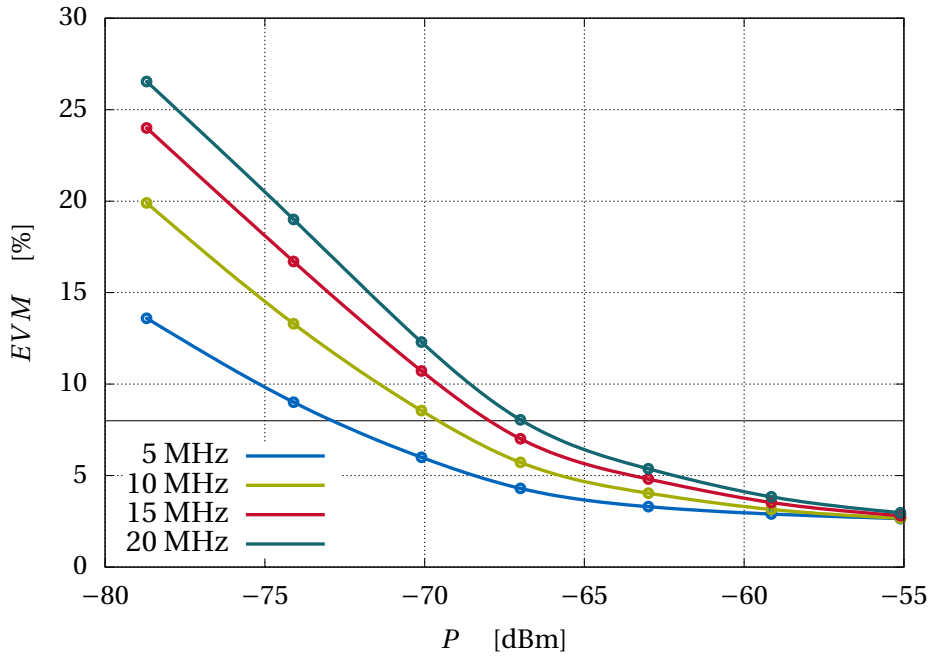

Figure 3.17: EVM as a function of received power level for 64-QAM with various bandwidths

EVM as a function of received power level for various types of modulations can be seen in Fig. 3.18 on the facing page (5 MHz bandwidth) and Fig. 3.19 on page 32 (20 MHz bandwidth).

The thresholds for the respective modulation are reached as follows:

	EVM	5 MHz	20 MHz	Difference
QPSK	18.5%	-76.0 dBm	-69.3 dBm	5.7 dB
16-QAM	13.5%	-75.7 dBm	-68.5 dBm	7.2 dB
64-QAM	9.0%	-74.1 dBm	-67.7 dBm	6.4 dB
256-QAM	4.5%	-61.5 dBm	-55.2 dBm	6.3 dB

Table 3.1: Modulation's performance

The EVM limits are reached, for the same bandwidth, sooner as as the modulation order increases. The difference is, however, not particularly large – outlier being 256-QAM. The extra power needed for the same quality transmission of 20 MHz modulation compared to 5 MHz is about 6 dB for all modulations.

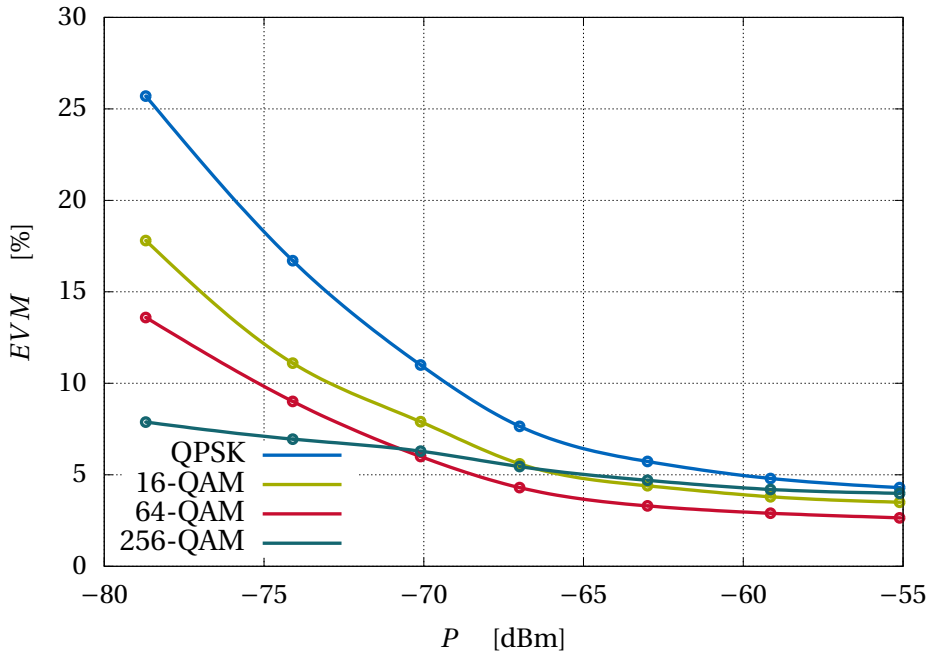

Figure 3.18: EVM as a function of received power level for 5 MHz modulations

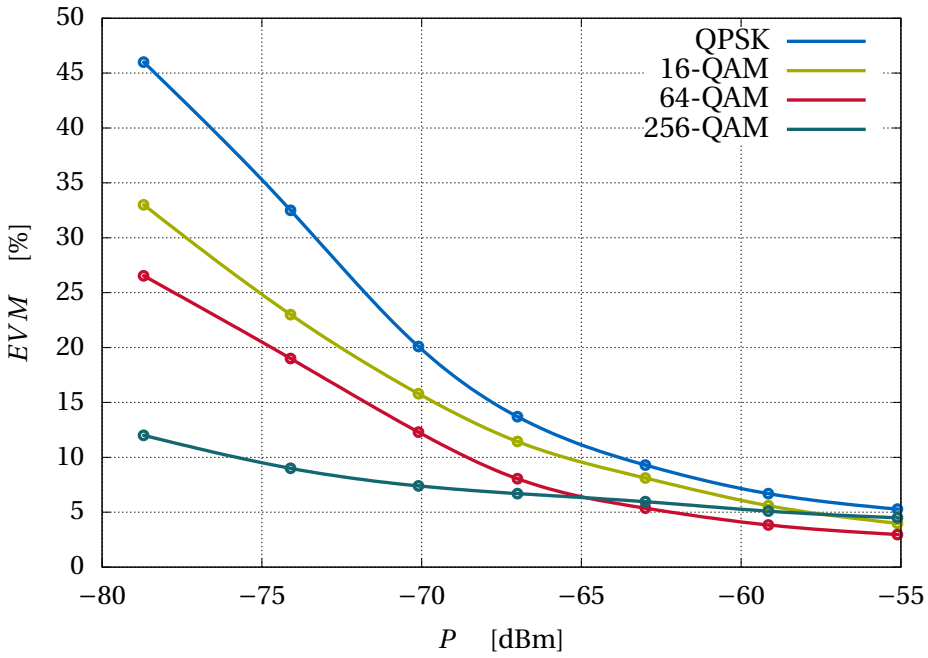

Figure 3.19: EVM as a function of received power level for 20 MHz modulations

3.5.4 Summary

Data transmission of a 25 GHz, 1550 nm RoF link with an optical channel was demonstrated. The phase noise of the carrier is increased by the optical channel only slightly (2.3 dB).

The signal quality of the link is largely influenced by the SNR (changed by the variable optical attenuator). As the bandwidth of the modulation increases its particular limit is reached at higher received power, as could be expected. However, the signal quality doesn't seem to degrade much as the number of modulation states increases. Their nominal thresholds are reached at similar power level – an outlier being 256-QAM which degrades more rapidly.

3.6 Measurement of Transmission through RoF Link with optical carrier suppression

Another goal was to measure behavior of the system under conditions mimicking actual full transmission channel. Also, carrier suppression was implemented with an additional MZM.

3.6.1 Setup

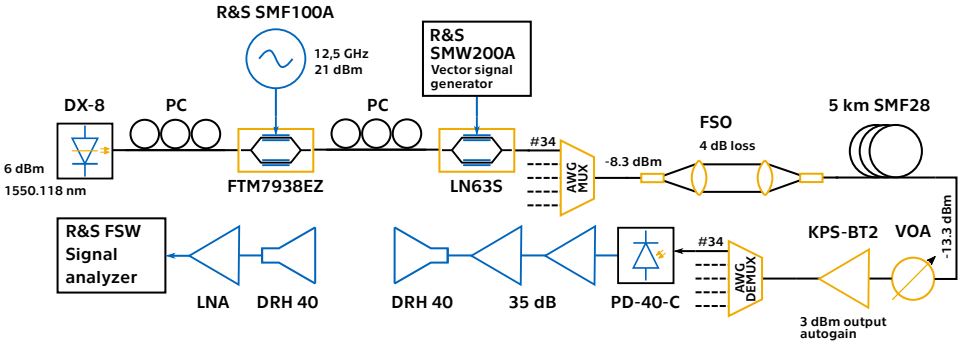

Figure 3.20: OCS link and measurement setup

See Fig. 3.20 for the setup's schematic, device configuration and power budget. Two MZMs were used for the OCS setup. The Fujitsu 40 Gb/s MZM was used as the LO modulator because of its wider bandwidth (see below for optical carrier suppression biasing), and a Thorlabs 10 Gb/s MZM (biased at 1.3 V maximum transmission point) was used as the IF modulator as the bandwidth of the IF signal doesn't go beyond 100 MHz. A radio link with previously mentioned DRH-40 antennas was added to mimic actual mobile downlink transmission. A DWDM multiplexer and demultiplexer was added to mimic conditions of an actual multiplexed optical transmission, although crosstalks were not measured.

See Fig. 3.20 for particular device configuration. The list of hardware used follows.

- Cobrite DX-4 DFB tunable laser
- Manual polarization controllers
- Fujitsu FTM7938EZ 40 Gb/s MZM (RF)
- Thorlabs LN63S 10 Gb/s MZM (IF)
- AWG multiplexer and demultiplexer
- Thorlabs fixed-focus collimators
- Keopsys KPS-BT2 EDFA
- PD-40-C PIN photodiode
- Set of mm-wave amplifiers (AMF-4F, HMC1131)
- DRH40 Double ridged horn antenna

The measurement devices are the same as in the simple RoF link measurement with some additions:

- Rohde & Schwarz SMF100A Microwave signal generator

- Rohde & Schwarz SMW200A Vector signal generator
- OZ Optics Digital variable optical attenuator
- Rohde & Schwarz FSW Signal and spectrum analyzer
- Yokogawa Optical spectrum analyzer

The three constituents of the link (5 km fiber, 2 m FSO, 3 m radio) were utilized and measured under three conditions.

Back to back Direct transmission

Optical link 2 m FSO and 5 km fiber

Full link Optical link plus 3 m radio link

The optical spectra were measured via a 20 dB fiber coupler. For ease of implementation, the baseband data was modulated upon a 50 MHz IF (the same fashion as it was done in the simulations) by the vector generator. The IF was modulated on the optical carrier by the Thorlabs LN63S MZM.

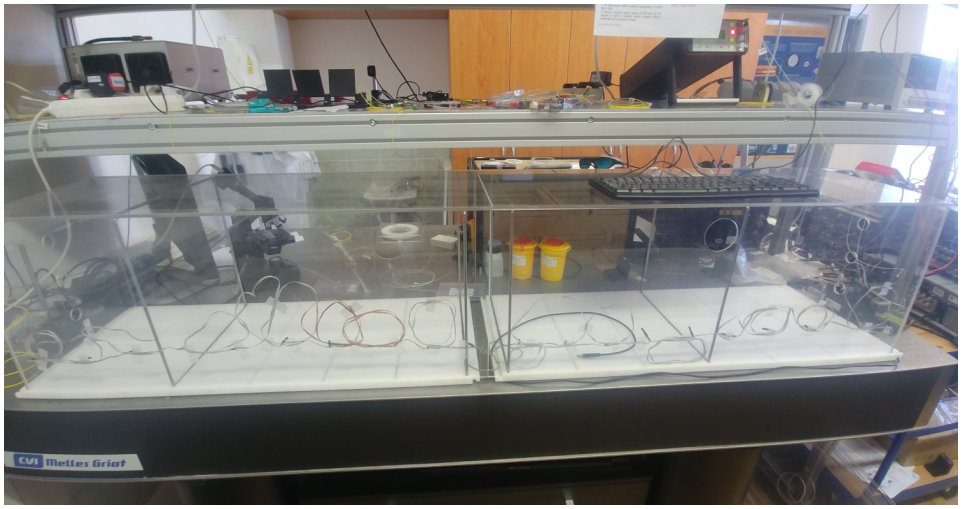

Figure 3.21: FSO link

3.6.2 Carrier Suppression Ratio

As the first step, the bias point of the LO MZM (Fujitsu) was set to achieve maximum optical carrier suppression ratio (*OCS*). The suppression ratios were measured via the optical spectrum analyzer (OSA) for various DC bias voltages and constant RF power (17 dBm). The best *OCS* of 22 dB was achieved at 3.4 V bias voltage. See Fig. 3.22 on the facing page for optical spectra after the LO MZM. The spectrum is similar to those simulated before (Fig. 3.5 on page 20) – both the fundamental wavelength and 2nd sidelobes are suppressed compared to the 2nd 12.5 GHz shifted sidelobes. For comparison two extra plots are added:

- A 7 GHz modulation showing tighter sidebands and potentially worse OCS, when the LO frequency is even lower

- A case with MZM biased badly for OCS showing worse conditions

The next step was to measure the dependency of RF modulation power on the carrier suppression and subsequently EVM of the transmission. This was measured in the Optical link setup with 64-QAM modulation and 20 MHz bandwidth (test model 3.1). The RF power going into LO MZM was varied while received EVM was measured on the signal analyzer while OCS was measured on the OSA. The results can be seen in Fig. 3.23 on the following page.

With increasing RF power we get roughly linearly increasing OCS, therefore it is desirable to modulate the MZM with a fairly strong LO signal as the MZM gets overdriven. In our case, the maximum RF power was limited by the generator's capabilities. However, with increasing RF power, hence OCS, the received EVM decrease has diminishing returns and tapers off at 2 %, so the advantage of having a strong RF signal doesn't translate directly received error magnitude and the OCS of about 15 dB seems to be sufficient.

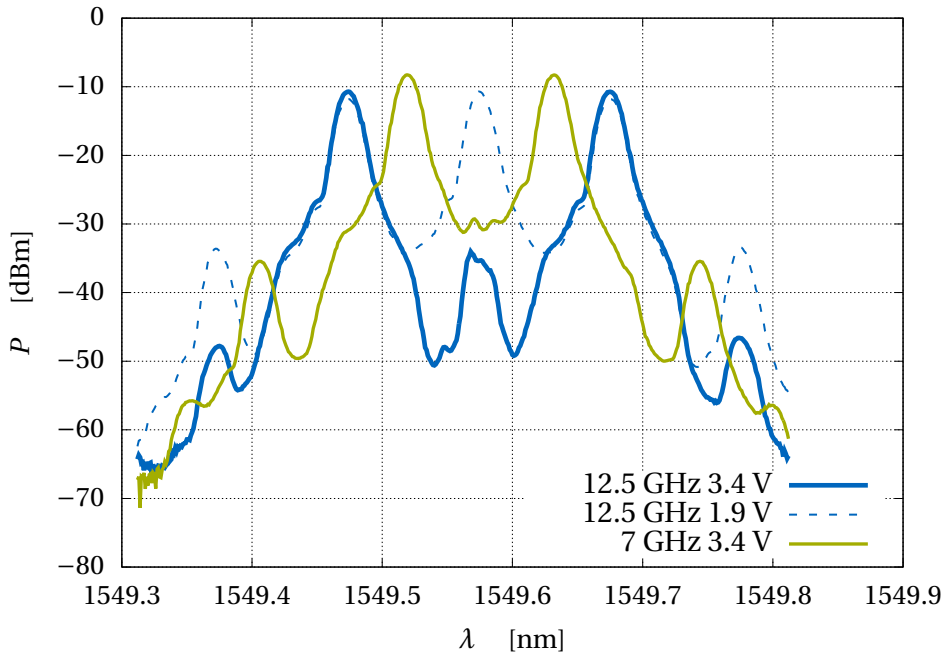

Figure 3.22: OCS measured optical spectrum

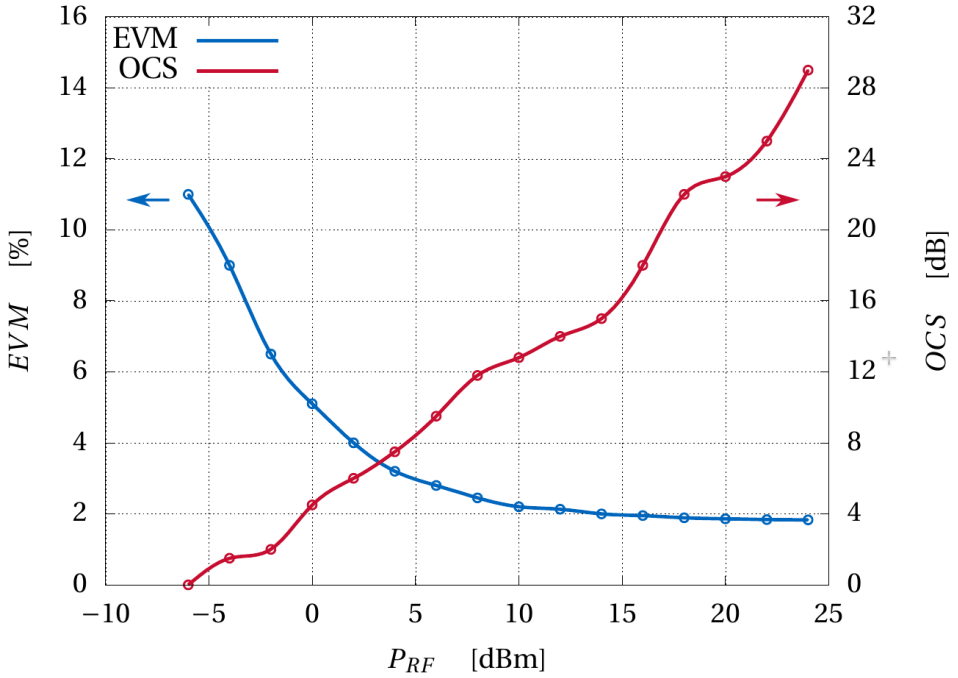

Figure 3.23: OCS and EVM as a function of RF power (64-QAM, 20 MHz, Optical link)

3.6.3 RF Domain

The RF spectrum of the detected signal with 20 MHz 64-QAM modulation can be seen in Fig. 3.24 on the next page. It shows the carrier frequency correctly multiplied at 25 GHz, with 50 MHz IF sidebands modulated with 20 MHz data on sufficient power level of -65 dBm. There are, however, intermodulation products offset by half of the IF frequency from the carrier. This limits the modulation bandwidth to 50 MHz – the IF frequency. This shows the limitations of this simple scheme as suggested in Sec. 3.1.2 on page 17. Modulating directly the carrier frequency of 12.5 GHz, hence also 25 GHz, would require more complicated baseband modulation at the second MZM.

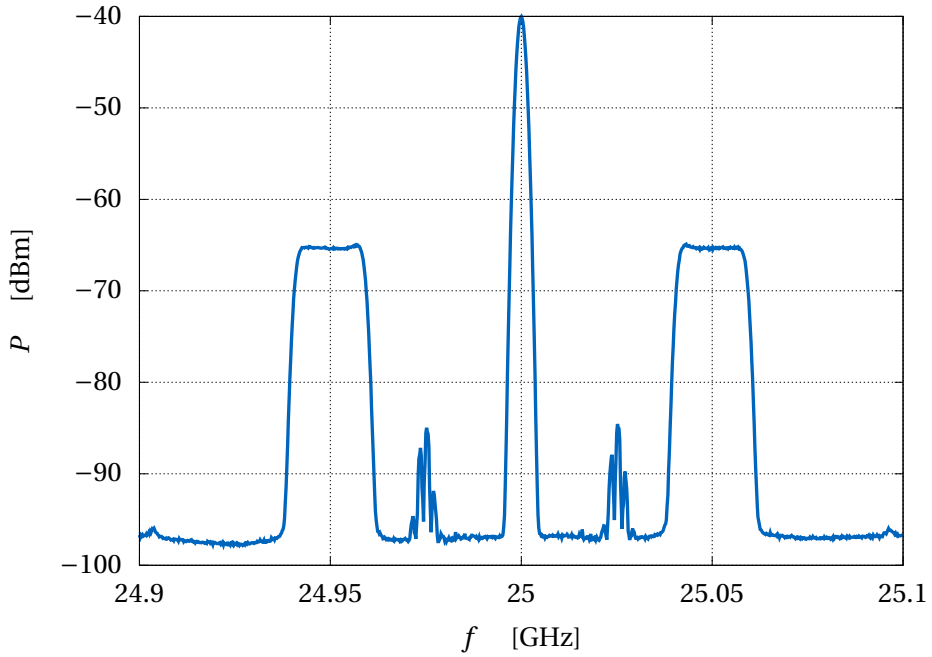

Figure 3.24: OCS link – measured RF spectrum

3.6.4 Modulation and Bandwidth

The EVM of the setup in the Optical link configuration was measured for various bandwidths with the same modulation. 64-QAM test schemes with bandwidths of 5, 10, and 20 MHz were used, constellation diagrams noted and EVM measured. The constellations show an ordinary behavior – as the SNR decreases, the detected pulses are more spread around the defined constellation points (see Fig. 3.25 on the next page for an example). EVM as a function of received power level for various bandwidth is depicted in Fig. 3.26 on the following page. The power level of the received signals was set by changing optical attenuation of the variable attenuator.

EVM as a function of received power level for 64-QAM with various bandwidths can be seen in Fig. 3.17 on page 30. The 8% threshold for 64-QAM nominal transmission is reached as follows:

5 MHz -71.6 dBm

10 MHz -68.6 dBm

20 MHz -65.9 dBm

These values are in fact very comparable to the measured in the previous setup without OCS (Sec. 3.5.3 on page 30).

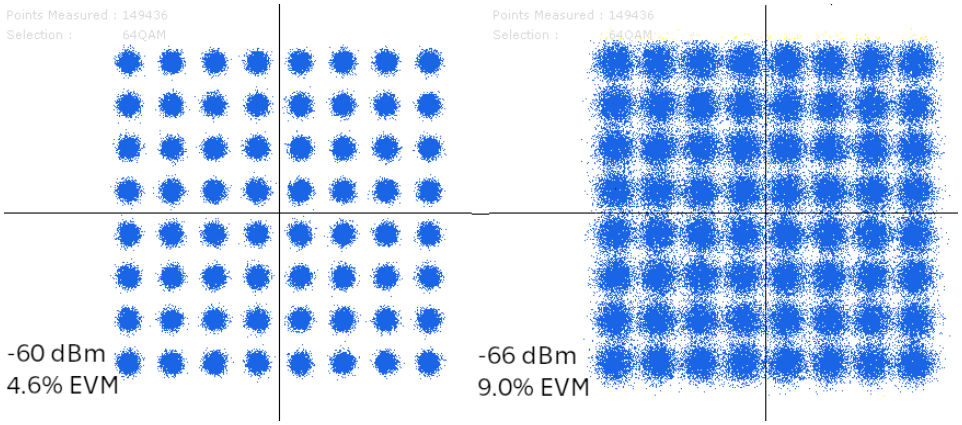

Figure 3.25: Constellations diagrams for 20 MHz 64-QAM, back to back link.

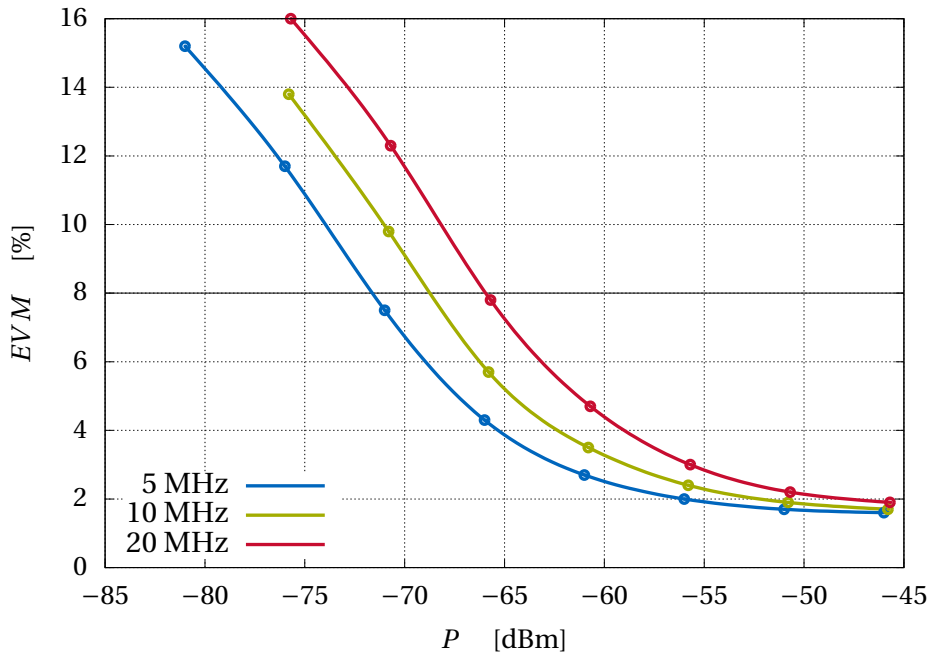

Figure 3.26: EVM as a function of received power level for 64-QAM with various bandwidths. OCS

Then, EVM as a function of received RF power level mas measured for QPSK, 16-QAM, and 64-QAM modulation for all three setups. The power level was again set by changing optical attenuation of the variable attenuator. See results in Fig. 3.27 on the next page for back to back setup, Fig. 3.28 on page 40 for optical link setup, and Fig. 3.29 on page 40 for full link setup. After E-UTRA base station conformance testing (3GPP TS 36.141 [25]) models, the EVM thresholds for nominal transmission are as noted before: QPSK: 17.5%, 16-QAM 12.5%, and 64-QAM 8%.

Across all modulations at a constant power level, Back to back setup shows best performance followed by optical link setup, and full link being weakest. Even though the power level is the same across the setups, the SNR gets worse by optical amplification of the EDFA and even worse by RF amplification after the radio link. As the SNR gets worse, EVM follows as well. For example, at -55 dBm of received power level, the EVM for 64-QAM is 3.5% for back to back link, 4.5% for optical link, and 12.5% for full link.

These values are very comparable to the values achieved in the previous, simpler setup, therefore any improvement due dispersion fading reduction because of OCS was not observed.

The SNR loss in the optical transmission channel is not as pronounced as the loss in the radio channel as the losses due to fiber attenuation and optical free space losses are much smaller than the radio free space losses. On the other hand, the performance across the modulations doesn't seem to change among the channels they are transmitted through – the nominal EVM value is crossed approximately at the same received power levels (-67 dBm for back-to-back, -64 dBm for optical link, and -53 dBm for full link).

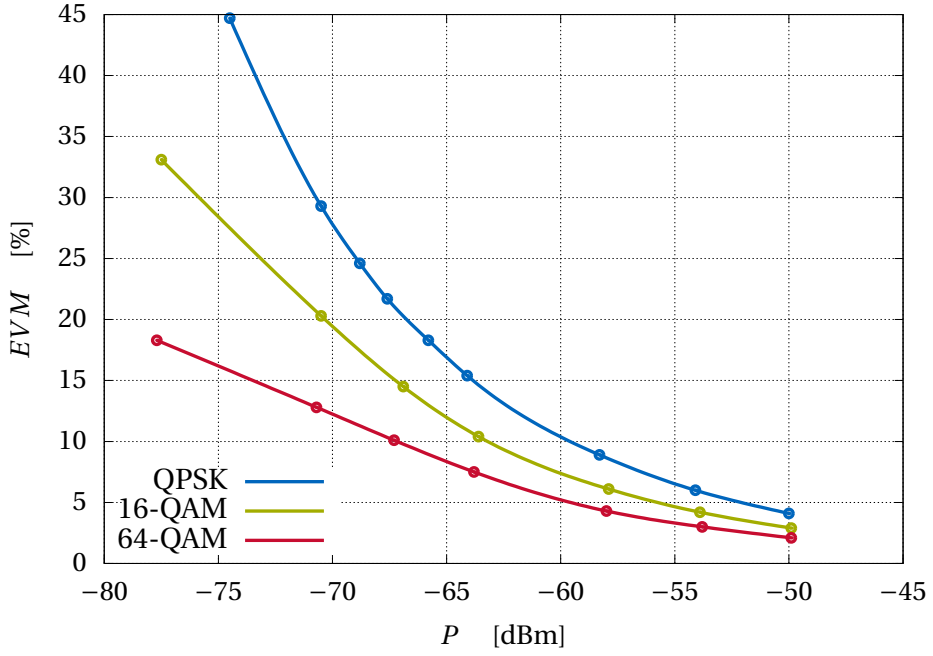

Figure 3.27: Back to back – EVM as a function of received power level for various modulations

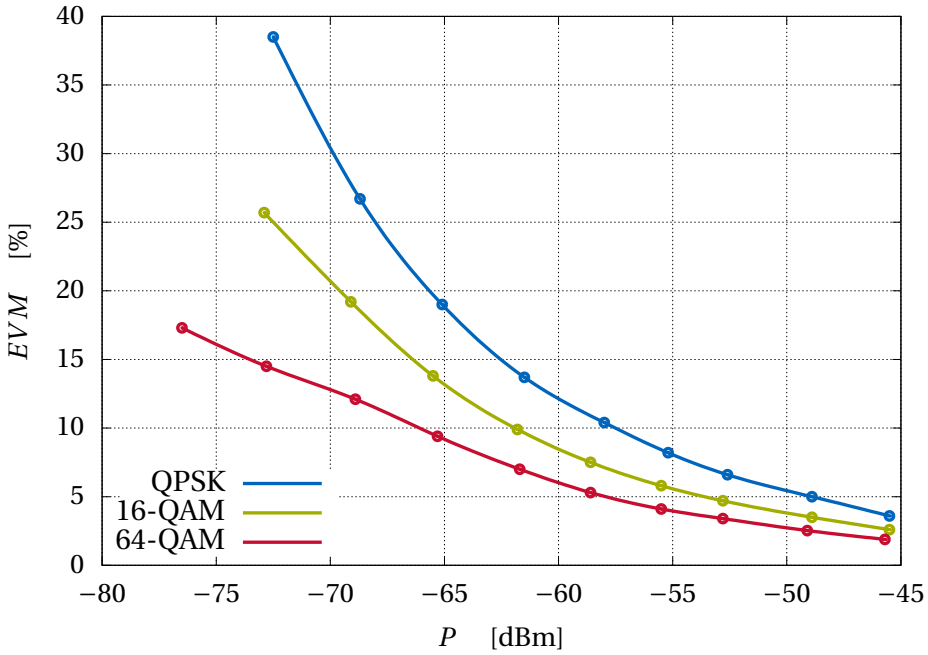

Figure 3.28: Optical link – EVM as a function of received power level for various modulations

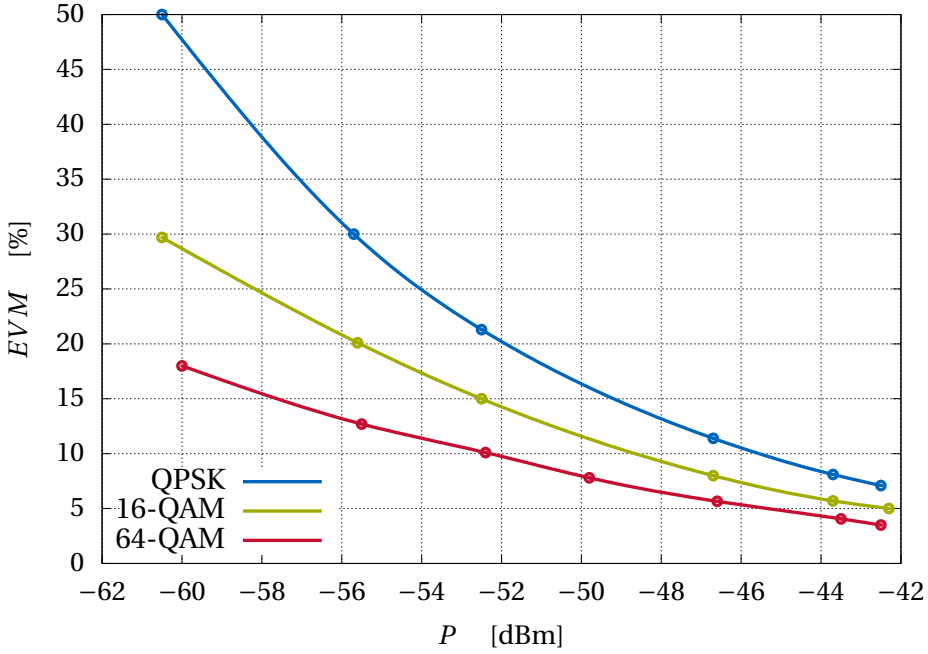

Figure 3.29: Full link – EVM as a function of received power level for various modulations

3.6.5 Summary

Data transmission of a 25 GHz, 1550 nm RoF link with optical carrier suppression and RF intermediate frequency was demonstrated.

OCS of 28 dB was achieved. It was shown that such high OCS is not needed as EVM doesn't improve much after OCS of about 15 dB is reached. The signal quality performance is similar to the case before, where no frequency multiplication is used. Improvement due to dispersion fading reduction was not observed. Most of signal degradation happens in the RF channel. An optical channel with FSO degrades the signal only slightly compared to the back to back case.

Part 4

Conclusion

General options for transmission of millimeter waves over fiber, particularly for 5G applications, were assessed.

Simulations were undertaken to demonstrate basic functionality of an RoF system with a MZM. Then optical carrier suppression transmission was demonstrated by setting the MZM to its null transmission point.

General hardware options for transmission of millimeter waves over fiber were considered with RoF being the simplest one. The choice of the modulator was considered with all MZM, EAM and DML being a viable option. However, MZM is needed for optical carrier suppression.

Then components of a RoF setup were measured on a RF vector network analyzer, that is a 40 GHz PIN InGaAs photodiode, a 40 Gb/s MZM, a 40 GB/s EAM integrated DFB laser and a buried heterostructure passive feedback DML. All the optical components show very good performance up to 30 GHz.

Then a functional RoF setup was measured on a RF vector network analyzer. For narrowband (carrier) transmission, the system's performance is mostly limited by radio components (amplifiers) although not to a great degree. The optical side of the system is not limiting.

Then an RoF data downlink without RF transmission was set up and measured. It showed good performance for QPSK, 16-QAM, 64-QAM and 256-QAM modulations and bandwidth up 20 MHz as per E-UTRA LTE base-station test models. The EVM limits for 20 MHz modulations were reached after additional 12 dB (64-QAM) to 14 dB (QPSK) detected RF signal attenuation. Only 256-QAM was close to the limit without any additional attenuation. Using 5 MHz modulation instead of 20 MHz modulations adds about 6 dB margin in the detected RF signal.

Then an optical carrier suppression link (implementing RF frequency doubling) with intermediate frequency was set up. It also included an FSO and radio channel. Optical carrier suppression ratio of 28 dB was achieved. It was shown that the optical channel doesn't degrade the signal as much as the RF channel. The degradation happens mostly because of additional attenuation and resulting SNR drop-off due to both optical and radio amplification. The performance was very similar to the simpler setup before.

References

[1] C. H. Lee, editor. *Microwave Photonics*. CRC Press, 2013.

[2] J. Campos. Understanding the 5G NR Physical Layer. Technical report, Keysight Technologies, November 2017.

[3] ITU. WRC-15: Studies on frequency-related matters for International Mobile Telecommunications identification including possible additional allocations to the mobile services on a primary basis in portion(s) of the frequency range between 24.25 and 86GHz for the future development of International Mobile Telecommunications for 2020 and beyond. *The World Radiocommunication Conference (Geneva, 2015)*.

[4] D. Tomimura. New Spectrum: Bands under Study for WRC-19. *ITU RRS-17 Americas*, September 2017.

[5] *Low Loss 086 Semi-Rigid Coax Cable, Copper Outer Conductor, Microporous PTFE 76.5 VoP Dielectric, Straight Sections*. Pasternack Enterprises Inc., 2018. Rev. 1.0.

[6] *SMF-28 Ultra Optical Fiber*. Corning Inc., November 2014.

[7] M. Sauer, A. Kobyakov, and J. George. Radio Over Fiber for Picocellular Network Architectures. *Journal of Lightwave Technology*, 25(11): 3301–3320, November 2007.

[8] D. Wake, M. Webster, G. Wimpenny, K. Beacham, L. Crawford, et al. Radio over fiber for mobile communications. In *2004 IEEE International Topical Meeting on Microwave Photonics*, pages 157–160, Oct 2004.

[9] J. Bohata, M. Komanec, J. Spáčil, Z. Ghassemlooy, S. Zvánovec, and R. Slavík. 24–26 GHz Radio-over-Fiber and Free-Space Optics for Fifth-Generation Systems. *Optics Letters*, 43(5), March 2018.

[10] J. Beas, G. Castañón, I. Aldaya, A. Aragaón-Zavala, and G. Campuzano. Millimeter-Wave Frequency Radio over Fiber Systems: A Survey. *IEEE Communications Surveys & Tutorials*, 15(4):1593–1619, 2013.

[11] L. Breyne, G. Torfs, X. Yin, P. Demeester, and J. Bauwelinck. Comparison Between Analog Radio-Over-Fiber and Sigma Delta Modulated Radio-Over-Fiber. *IEEE Photonics Technology Letters*, 29(21):1808–1811, November 2017.

[12] I. Gasulla and J. Capmany. Phase-modulated Radio Over Fiber Multimode Links. *Optics Express*, 20(11), May 2012.

[13] Radio-over-fibre (RoF) technologies and their application. *ITU-T, Series G, Supplement 55*, July 2015.

[14] N. J. Gomes, P. P. Monteiro, and A. Gameiro, editors. *Next Generation Wireless Communication Using Radio over Fiber*. Wiley & Sons, 2012.

[15] L. A. Johansson and A. J. Seeds. Generation and transmission of millimeter-wave data-modulated optical signals using an optical injection phase-lock loop. *Lightwave Technology, Journal of*, 21:511–520, 03 2003. doi: 10.1109/JLT.2003.808747.

[16] J. Park, M. S. Shakouri, and K. Y. Lau. Millimetre-wave electro-optical upconverter for wireless digital communications. *Electronics Letters*, 31(13), June 1995.

[17] R. S. Tucker. High-Speed Modulation of Semicoductor Lasers. *Journal of Lightwave Technology*, LT-3(6):1180–1192, December 1985.

[18] R. Hui and M. O'Sullivan. *Fiber Optic Measurement Techniques*. Elsevier, 2009.

[19] C. K. Sun, R. J. Orazi, and S. A. Pappert. Efficient Microwave Frequency Conversion Using Photonic Link Signal Mixing. *IEEE Photonics Technology Letters*, 8(1), January 1996.

[20] J. Zhang, H. Chen, M. Chen, T. Wang, and S. Xie. A Photonic Microwave Frequency Quadrupler Using Two Cascaded Intensity Modulators With Repetitious Optical Carrier Suppression. *IEEE Photonics Technology Letters*, 19(14), July 2007.

[21] S. Yu, W. Gu, A. Yang, T. Jiang, and C. Wang. A Frequency Quadrupling Optical mm-Wave Generation for Hybrid Fiber-Wireless Systems. *IEEE Journal on Selected Areas in Communications*, 31(12): 797–803, December 2013.

[22] O. Bouchet, H. Sizun, C. Boisrobert, F. de Fornel, and P.N. Favennec. *Free-Space Optics, Propagation and Communication*. ISTE, 2006.

[23] J. Kreissl, V. Vercesi, U. Troppenz, T. Gaertner, W. Wenisch, and M. Schell. Up to 40-Gb/s Directly Modulated Laser Operating at Low Driving Current: Buried-Heterostructure Passive Feedback Laser (BH-PFL). *IEEE Photonics Technology Letters*, 24(5), March 2012.

[24] E-UTRA Base Station (BS) Radio Transmission and Reception. *3GPP TS 36.104*, March 2019.

[25] E-UTRA Base Station (BS) conformance testing. *3GPP TS 36.141*, March 2019.

[26] Keysight Technologies. Error Vector Magnitude (Digital Demodulation). `http://rfmw.em.keysight.com/wireless/helpfiles/89600b/webhelp/subsystems/digdemod/Content/digdemod_symtblerrdata_evm.htm`. Accessed: 2019-05-20.

[27] R. J. Collier and A. D. Skinner, editors. *Microwave Measurements*. The Institution of Engineering and Technology, 2007.

[28] *R&S SMF100A Microwave Signal Generator*. Rohde & Schwarz, 2016. Rev. 05.01.

List of Figures